

Simulation and Analysis of the Code Domain NOMA with UFMC for 5G Wireless Networks

Smita Jolania* (*Research Scholar, IET, DAVV, Indore, India*)

Ravi Sindal (*Professor, IET, DAVV, Indore, India*)

Ankit Saxena (*Associate Professor, Indore Institute of Science and Technology, Indore, India*)

Abstract – In fifth generation (5G) wireless networks, radio access techniques and multi-carrier waveforms play a vital role in meeting the diversified demands of ultra-low latency, massive connectivity, and higher throughput. Multi-access schemes used conventionally in 4G system was Orthogonal Multiple Access (OMA) technique. The OMA techniques suffer from inefficient spectrum utilization, high latency, and supports a limited number of users. Next-generation networks, Non-Orthogonal Multiple Access (NOMA), has a great potential, in which multiple users are simultaneously served using the same time, frequency, or code resource increasing the throughput. Code domain-NOMA (CD-NOMA) is the key technique implemented in the system design where multiple users are distinguished based on unique user-specific spreading codes. The NOMA system could significantly benefit from Universal Filtered Multi-Carrier (UFMC) modulation waveform in terms of flexibility, spectral efficiency, compatibility with Multiple Input Multiple Output (MIMO) technique, and relaxed synchronization requirements. The novel integrated system proposed in the paper is CD-NOMA-UFMC with convolutional codes. The major outcome of the paper is that the combination of UFMC air interface modulation technique with CD-NOMA access method can be the most effective way to meet the growing demands of 5G.

Keywords – CD-NOMA, convolutional codes, UFMC.

I. INTRODUCTION

The next-generation mobile communication networks must deliver advanced services like augmented reality (AR) and virtual reality (VR) with efficient bandwidth usage to support them. Major 5G use cases need to support ultra-dense networks with diverse end-to-end connectivity. The heterogeneous needs like extremely high speed, reliability, user fairness, and low latency are to be addressed in system design [1]. The use cases in 5G are enhanced mobile broadband (eMBB) to provide a high data rate at gigabits per second, ultra-reliable low latency communications (URLLC) to optimize throughput and delay with latency less than 1 ms [2]–[4]. Another use case is massive machine-type communications (mMTC), where huge number of devices with small data packets is connected [5]. It is very challenging to facilitate all these requirements and design an optimized system in the context of spectrum utilization and throughput.

In the view of spectrum scarcity, it becomes crucial to identify the techniques focused on efficient spectrum

management to meet the massive device connectivity and huge data rate. Effective utilization of the available spectrum needs to enhance the network architecture with some emerging technologies proposed in [6]. As seeing the limited spectrum, multiple access (MA) schemes are to be applied for efficient radio resource management. MA schemes mainly serve the users by sharing the radio resources and discriminating the user channels based on time, frequency, or code [7]. In Orthogonal Multiple Access (OMA) schemes, resource blocks orthogonal either in time, frequency, or code domains are allocated to users [8]. The OMA is effective when the number of active users is less than the number of block resources. Non-orthogonal multiple access (NOMA) is a promising technique and envisioned as a key component in 5G mobile systems to serve a larger number of active users with efficient utilization of available resources [9]. In NOMA, non-orthogonal resource blocks are allocated to serve multiple users. The NOMA scheme allows the Next Generation Node B (gNB) to simultaneously serve all users by using the entire bandwidth to transmit data. To deal with interference at the receiver side, different users are detected based on the difference of power or spreading codes, leading to two main corresponding approaches: power-domain NOMA (PD-NOMA) and code-domain NOMA (CD-NOMA). The concept of NOMA emerged from PD-NOMA, so let us understand the concept of PD-NOMA and its limitations, which further leads to CD-NOMA.

In PD-NOMA, different signals generated by different users at the same time or frequency block are combined using superposition coding (SC) at the BS. The superposition is done with different allocated power coefficients to all mobile users. Power coefficients of users are allocated according to their channel conditions, in an inversely proportional manner. The SC is a technique of simultaneously communicating information to several receivers by a single source [10], [11]. In downlink PD-NOMA network, for decoding, the user with a stronger channel gain uses successive interference cancellation (SIC). The process involved in decoding the superimposed messages is analysed mathematically in [12], to decode its signal free of interference. The user with weaker channel gain treats the signals of the stronger users as noise [13]. To achieve the superior spectral efficiency of NOMA, energy efficiency

*Corresponding author. E-mail: sprajapati2911@gmail.com
Article received 01-08-2023; accepted 12-12-2023

and user fairness need to be focused on the power allocation, in PD-NOMA [14]. Seyed Hadi et al. [15] presented the technique to maximize the energy efficiency, spectral efficiency, and total transmission power in PD-NOMA particularly in the scenario of unmanned aerial vehicles (UAVs). The limitation for power-based NOMA is that the non-orthogonal transmission receiver is rather complex; SIC receiver design requires significant improvement in signal processing aspects. Also, when an error occurs in SIC at a user, the subsequent decoding of all other users' information will likely be carried out erroneously [15].

CD-NOMA has gain of shaping flexibility with the cost of bandwidth of signal compared with simple PD-NOMA [16]. CD-NOMA is the prime focus of the proposed system, where the multiple users communicate at the same time and frequency resource block but are differentiated by codes. Unique spreading codes play the major role in CD-NOMA technique. The major benefits of CD-NOMA technique are enhanced spectrum efficiency and improved system capacity [17]. To further escalate the spectrum utilization, new waveform Universal Filtered Multi-carrier (UFMC) is implemented in the network. In UFMC, sub-band filtering is applied where the total bandwidth is divided into number of sub-bands, and filtering is applied in the frequency domain to reduce out-of-band (OOB) emissions. Due to fine frequency filtration, shorter filter length, and compatibility with MIMO, UFMC is one of the most suitable multicarrier waveforms for 5G [18], [19].

The comprehensive system of CD-NOMA-UFMC proved to provide better power efficiency. Additionally, motivated from the results obtained in [21] where the combination of multicarrier waveform and forward error correction are implemented, convolutional codes in UFMC are integrated for enhancing the BER performance of the designed system. Moreover, the system can be extended for Multiple Input Multiple Output (MIMO) as presented in [22], large antenna array scenario for enhancing the data rate and user density.

II. SYSTEM MODEL

The study proposes a novel integrated system CD-NOMA and UFMC with channel coding. The comprehensive transceiver for the proposed system can be explained by dividing it into different sub-blocks: (i) convolution coding, (ii) CD-NOMA technique, (iii) UFMC modulation, (iv) Rayleigh channel, and (v) receiver (including zero-forcing detection, channel decoding, multi-user detection (MUD), and UFMC demodulation). In the proposed system, the symbols are firstly encoded using convolution coding and then spread by a user signature code. Then the data symbols are modulated in each sub-band as per UFMC. The block diagram of the comprehensive transmitter for j^{th} user CD-NOMA-UFMC system with convolution coding over the Rayleigh channel is depicted in Fig. 1.

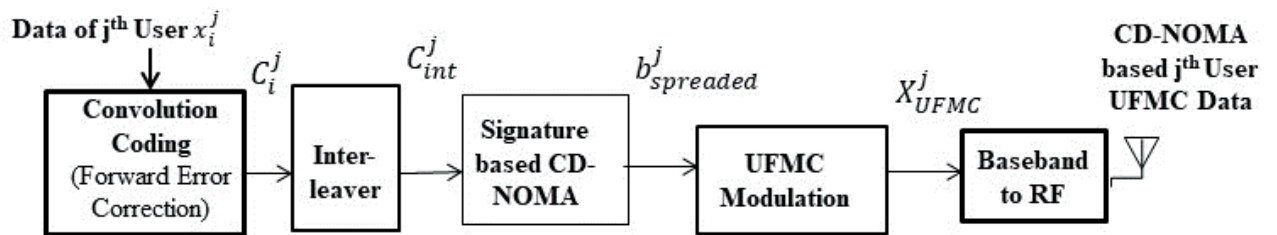


Fig. 1. Convolution coded CD-NOMA-UFMC transmitter block.

With reference to the system design proposed in [20], which combines the CDMA and FBMC with cosine-modulated filter banks, here the system is proposed combining CD-NOMA and UFMC. The objective of implementing CD-NOMA has two advantages. One is to reduce interference by spreading the data symbol in each sub-band and to support multi-user communication to differentiate the users based on signature code. After the rigorous literature survey, it has been concluded that the combination of the CD-NOMA and UFMC with convolution coding was not considered previously in the literature. The list of symbols used in the paper is provided in Table I.

TABLE I
LIST OF SYMBOLS USED IN THE PAPER

Symbol	Designation
j	User index
x_i^j	Generated data blocks

$c_{i,j}$	Channel encoded data
C_{int}^j	Data after interleaving
k	Number of encoded information bits
n	Number of encoded bits
R	Code rate (k/n)
K	Constraint length
D	Flip-flop state in convolution encoder
$g(x)$	Generator polynomial
$b_{spreaded}^j$	Spread data symbol
$s_j(t)$	QAM symbols in the frequency domain
β	Total number of subcarriers
B	Number of sub-bands
Q	Number of sub-carriers

$Q_i = Q/B$	Subsequent subcarriers in the i^{th} sub-band
$s_{j,i}(t)$	QAM symbol in the i^{th} sub-band
N	IFFT size
$y_{j,i}$	Time-domain symbol (after IFFT)
f_i	Prototype filter response
L	Filter length
α	Filter side-lobe attenuation
X_{UFMC}^j	UFMC resultant symbol of the j^{th} user
H	Channel matrix
X	Transmitted vector
Y	Received vector
η	AWGN noise vector
M	Order of QAM
y_1, y_2	The signal received at receiver 1 and receiver 2
\hat{x}_{2N}	Expected frequency domain symbol
F_i	Filter response matrix
V_i	IFFT matrix
\hat{x}_j	The detected symbol for the j^{th} user

A. Convolutional Coding

A random data source generates random bits for each user. Let x_i^j be the i^{th} data symbol transmitted from the j^{th} user. These data bit streams are encoded with convolutional coding to get c_{ij} for the j^{th} user. In convolution coding, k consecutive bits are encoded into a sequence of n bits. The code rate is evaluated as $R = k/n$, and the constraint length K is defined as the number of k bits that affect the formation of encoded n bits. The convolution encoder uses shift register of length K [23]. The channel encoder used in the proposed system is shown in Fig. 2. The encoded bit stream can be represented by (1):

$$C_{i,j}^{(m)} = \sum_{u=0}^2 D_i - u g_u^{(m)}, \quad (1)$$

where D represents flip flop (memory element), the relation of output bits to inputs is expressed using generator polynomials $g(x)$ and can be written as (2) and (3):

$$g^{(1)}(x) = 1 + x; \quad (2)$$

$$g^{(2)}(x) = 1 + x + x^2. \quad (3)$$

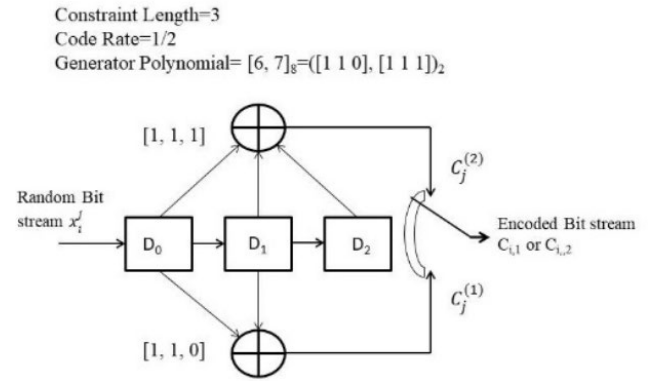


Fig. 2. Convolution encoder.

The interleaver is applied to disperse the sequences of bits in the encoded bit stream to minimize the effect of burst errors. The encoded data stream is interleaved by using random interleaver to get the resultant bit stream represented as C_{int}^j [24].

B. CD-NOMA Block

CD-NOMA technique is applied where each user will use a signature code to spread the data, and the receiver decodes it by using the same code. The principle of CD-NOMA is illustrated in Fig. 3.

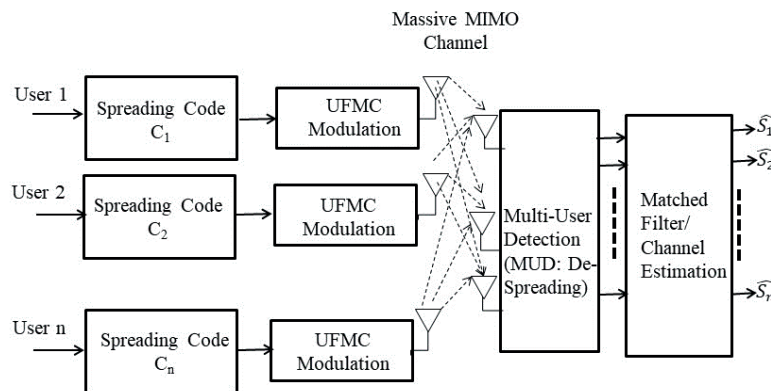


Fig. 3. CD-NOMA transceiver block [23].

Channel-encoded and interleaved data from the users are then spread using the unique signature chip to generate a spreading sequence. Existing CD-NOMA solutions include low density spreading CDMA (LDS-CDMA), LDS-OFDM, sparse code multiple access (SCMA), interleave division

multiple access (IDMA), etc. In the proposed system LDS-CDMA code scheme is implemented. The spreading sequences are provided to each user and are known to receiver. Figure 4 shows the LDS structure to generate the spreading sequences. Let us say that the length of spreading sequence

(chip length) is N . In conventional CDMA, all the N chips are non-zero while in the proposed LDS structure, the N chips are arranged in such a way that each user spreads their data over a small number of chips d_v . Then, zero padding is applied and the chips are interleaved in such a way that the resultant spreading sequence matrix becomes sufficiently sparse. The resultant spreading sequence will have d_v non-zero values and $(N-d_v)$ zero values. Chip level soft-in soft-out multiuser detection using message passing algorithm is used for detecting the LDS spreading sequence. The performance evaluation of LDS based CDMA system is presented in [25], which proved that the performance of LDS-CDMA is far better than conventional CDMA.

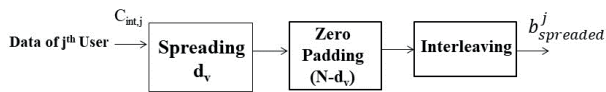


Fig. 4. LDS structure.

At the spreader, the encoded information bits C_{int}^j are spread in the time domain by the j^{th} user's spreading sequence. Each user is assigned a unique c -bit chip sequence C_{seq}^j to the j^{th} user. Here the number of bits in the spreading code or chip sequence is called a spreading factor. The spreading code must be unique for each user. The resultant spread data bits for the j^{th} user are represented as $b_{spreaded}^j$.

C. UPMC Modulation

Multi-carrier modulation (MCM) is performed after spreading the encoded data of each user. In MCM, the high data rate stream is divided into various sub-streams with a

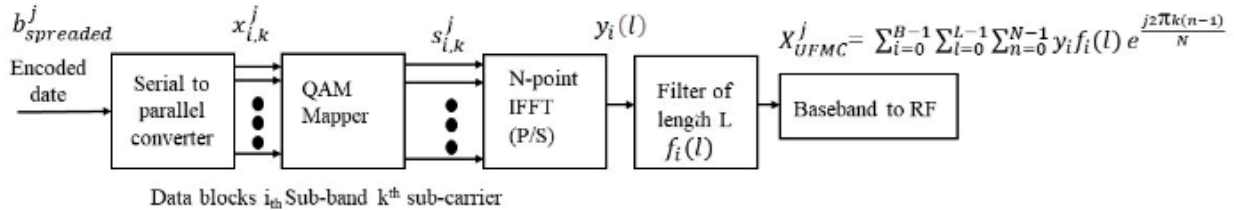


Fig. 5. UPMC modulator block.

Let us assume that the total bandwidth available for each user is β . This bandwidth is divided into Q number of subcarriers indexing from $[0, 1, 2, \dots, Q-1]$. In UPMC, all the allocated sub-carriers are grouped into several sub-bands indexing from $[i = 1, 2, \dots, B]$. For the i^{th} sub-band, with each including Q_i subcarriers mean Q subcarriers in the i^{th} sub-band ($\sum_{i=1}^B Q_i = \beta$). For the i^{th} sub-band, the QAM symbols for j^{th} are represented with $s_{j,i}(t)$. The n_i complex frequency domain QAM symbols for each user are transformed to time-domain by N -point IFFT module. The IFFT equation is as follows:

$$y_i(l) = \frac{1}{\sqrt{N}} \sum_{k=0}^{Q_i-1} s_{j,i}(k) e^{j2kl/N}, \quad (4)$$

lower data rate. These low data rate sub-streams are modulated on different sub-channels. After mapping, these sub-channels are multiplexed in the frequency domain. The proficient multi-carrier waveforms for 5G wireless networks are Filtered Orthogonal Frequency Division Multiplexing (F-OFDM), Universal Frequency Division Multiplexing (UFMC), Filter Bank Multi Carrier (FBMC), and Generalized Frequency Division Multiplexing (GFDM) [26]–[30]. FBMC and GFDM perform subcarrier-wise filtering but do not support backward compatibility and need a new transceiver design [26]. Although FBMC is one of the reliable methods as far as BER performance is considered, but it is incompatible with MIMO applications. In terms of BER performance, as seen from [31], UFMC outperforms OFDM and GFDM. UFMC is based on sub-band wise filtering, so it requires simple equalization procedures, and a smaller filter length when compared to FBMC and GFDM. Shorter filter lengths in UFMC as compared to the subcarrier-wise filtering techniques make it more suitable for low-latency applications [32].

The UFMC is the most prominent modulation proposed for the 5G communication network that is based on sub-band filtering technique, where filtering is performed with a fixed granularity of frequency domain [33]. The block diagram of the UFMC transmitter is depicted in Fig. 5. In the UFMC modulation, firstly, the serial data stream is converted to a parallel stream. The resultant sub-streams are QAM modulated and fed to the N point Inverse Fast Fourier Transform (IFFT) section to transform the frequency domain QAM samples to the time domain. The resultant time domain signal is further serialized block-wise and filtered to form UFMC signal [34].

where k is the sub-carrier index in the i^{th} sub-band. Then, sub-band filtering is performed by prototype filter of length ' L ', and α as side lobe attenuation, and generally each filter power is normalized to unity and mathematically expressed by (5):

$$\sum_{l=0}^{L-1} |f_i(l)|^2 = 1. \quad (5)$$

The time domain signal is filtered using the Dolph-Chebyshev filter of length L . The resultant UFMC signal for the j^{th} user is shown in (6) as follows:

$$X_{UMPC}^j = \sum_{i=1}^B y_i(l) * f_i(l), \quad (6)$$

where $l = 0, 1, \dots, N + L - 2$. Here ‘*’ symbolizes linear convolution. Finally, a complex UFMC signal can be represented by (7):

$$X_{\text{UFMC}}^j = \sum_{i=0}^{B-1} \sum_{l=0}^{L-1} \sum_{n=0}^{N-1} y_i f_i(l) e^{\frac{j2k(n-1)}{N}}. \quad (7)$$

This generated UFMC modulated signal is transmitted from j^{th} user.

D. Wireless Rayleigh Channel

The A channel model is to be considered to properly estimate the signal at the receiver end. In the proposed system, two users are transmitting the convolution coded CD-NOMA-UFMC signal, and, at the receiver, the signal is detected after passing through the Rayleigh channel. As shown in Fig. 6, the receiver antenna receives the direct signal intended for it and a fraction of the signal propagated from another user. Thus, the channel matrix H represents the channel response:

$$Y = HX + \eta, \quad (8)$$

where H is the channel matrix, $X \in \mathbb{C}^2$ denotes the transmitted signal, $Y \in \mathbb{C}^2$ is the received signal; $\eta \sim \text{CN}(0, R_n)$ complex Gaussian vector of white Gaussian noise with zero mathematical expectations and a correlation matrix R_n . Here \mathbb{C} symbolizes a complex channel.

Let y_1 and y_2 be the received symbol on the first and second received antenna, respectively, and the channel matrix

$H \in 2 \times 2$ is deterministic and assumed to be always constant and known to both the transmitter and the receiver. The channel comprises complex Gaussian random variables with zero mathematical expectations and unit variance for Rayleigh fading. The channel is a Rayleigh channel with channel gain ($|h_{ij}|$). The matrix form is shown in (9):

$$\begin{bmatrix} y_1 \\ y_2 \end{bmatrix} = \begin{bmatrix} h_{11} & h_{12} \\ h_{21} & h_{22} \end{bmatrix} \begin{bmatrix} x_{\text{UFMC}}^1 \\ x_{\text{UFMC}}^2 \end{bmatrix} + \begin{bmatrix} n_1 \\ n_2 \end{bmatrix}. \quad (9)$$

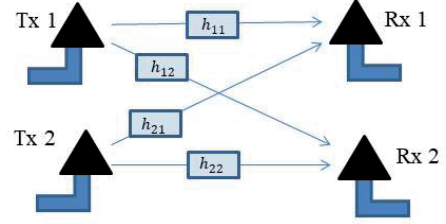


Fig. 6. Rayleigh channel model.

E. CD-NOMA-UFMC Receiver

After transmitting UFMC modulated signal from both the users through the Rayleigh channel, the RF signal is received at the receiver end. The block diagram of the receiver is depicted in Fig. 7.

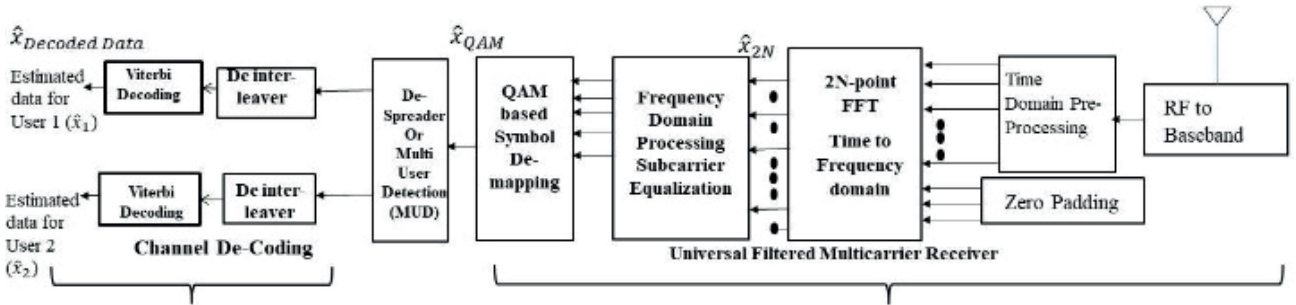


Fig. 7. UFMC CDMA receiver block.

At the receiver, channel equalization is applied. After the RF-link section, the signal will pass through the time domain pre-processing window to suppress interference. As a UFMC symbol has a length $(N+L-1)$, its conversion from the time domain to the frequency is performed using a $2N$ -point FFT, and the missing samples $N-L-1$ is padded with zeros. $2N$ point FFT is considered to recover the data to transfer in the frequency region. $2N$ -point FFT produces N output spectral lines represented as \hat{x}_{2N} . The demodulated signal after FFT is equalized and processed in the frequency domain, then sent to the de-mapper, which is a QAM demodulator to retrieve the data bits from the received symbols. After de-mapping the retrieved symbols are de-spread by using the user signature code. Then channel decoding is done for recovering the encoded input data stream, and here the maximum likelihood decoding is applied, which is also termed Viterbi decoding. The

Viterbi decoding algorithm comprises two metrics: the branch metric (BM) and the path metric (PM). In this method, decoding time is fixed, and it is decided based on these metrics. The key point in this technique is that the receiver computes the PM for a (state, time) pair sequentially using the PM of previously computed states and the BM [35]. Finally, at the receiver end, User1 and User2 data are estimated a \hat{x}_1 , and \hat{x}_2 .

III. SIMULATION AND RESULTS

The complete system is designed and simulated in MATLAB 2022b version. We have considered the multi-user scenario with the number of users assumed to be 2, the response of UFMC in the Rayleigh fading channel for 16 QAM is presented in Fig. 8 for a total number of subcarriers $P = 200$.

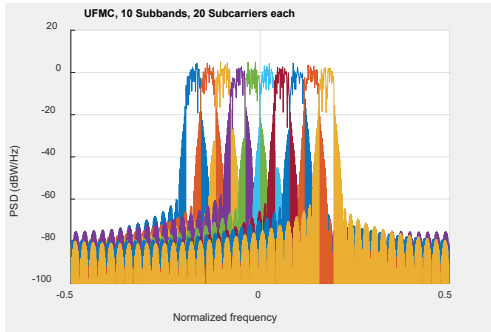


Fig. 8. PSD of UPMC.

TABLE II
SIMULATION PARAMETERS

Sub-blocks/Technique	Parameter	Value
UPMC Waveform Modulation	Number of sub-bands (B)	10
	Number of sub-carriers in each Sub-band (Q)	20
	Sub-band offset	156
	Modulation type (M) QAM	16
	Size of IFFT (N)	512
	Filter	Dolph-Chebyshev
	Filter length (L)	43
	Side lobe attenuation (α)	40 dB
Channel Coding	Channel coding	Convolution
	Code rate (R)	1/2
	Constraint length	3
	Code generator	[6 7]
	Channel decoding	Viterbi Decoding Hard Decision
CD-NOMA	Chip rate	8

UPMC waveform is simulated with different system parameters and the performance parameters. Power spectral density (PSD) and BER are analysed. In the proposed system, FIR filter designed using the Dolph-Chebyshev window is used for filtering in UPMC. Figure 8 shows the normalized spectrum of the UPMC system with 10 sub-bands having 20 subcarriers.

Firstly, UPMC modulation is simulated for different QAM modulation order using the Dolph-Chebyshev filter. The peak-to-average-power ratio (PAPR) is evaluated and the BER curve is obtained as shown in Fig. 9. Since we have implemented the UPMC modulation technique which is compatible with the QAM technique and higher order QAM supports in improving data rate at the cost of BER loss.

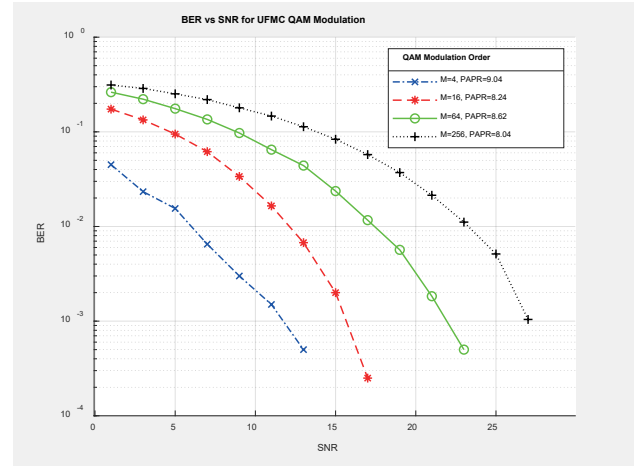


Fig. 9. BER performance for UPMC at higher order QAM.

It can be concluded from Fig. 10, BER curve simulated for 64QAM modulation order with 200 sub-carriers, at SNR = 15 dB, in the UPMC waveform BER achieved is 4×10^{-3} while in the CD-NOMA-UPMC waveform at the same SNR, the value of BER achieved is 4×10^{-4} . Hence, the BER performance improves with CD-NOMA implementation.

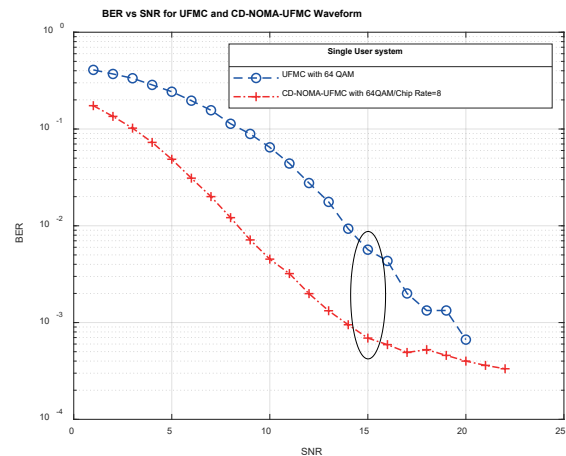


Fig. 10. BER performance comparison for CD-NOMA-UPMC and UPMC at 64QAM.

Figure 11 shows the performance of the CD-NOMA-UPMC system in a multi-user scenario with chip rate 8 using convolution codes and transmitted through the Rayleigh channel. It reveals that the performance of the proposed system was considerably enhanced than that of the un-coded system. Thus, using convolution code in the CD-NOMA-UPMC system contributes to enhancing BER performance, where the errors go to zero at 12 dB SNR for User 1 and 14-dB SNR for User 2 for the proposed system against an un-coded system where BER is very high.

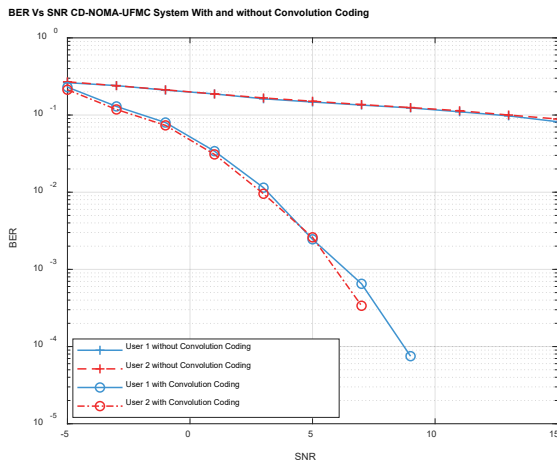


Fig. 11. BER performance of UPMC-CD-NOMA in a multiuser scenario.

The simulated system can be further extended in a large-scale MIMO system called Massive MIMO to enhance the data rate, the quality of services, energy efficiency, and spectral efficiency [36]. However, the detector should be designed for optimal performance as the number of users increases.

IV. CONCLUSION

In the paper, simulation, and analysis of a CD-NOMA-UPMC system was proposed. The proposed system uses convolution codes as they are much easier to implement and able to handle a continuous bit stream. The results proved that the BER performance of convolution coded UPMC waveform had better performance as compared to the un-coded waveform. Also, higher-order QAM supported by UPMC enhanced the data rate. The work concluded that UPMC provided flexibility about the choice of filter characteristics, sub-band size, and FFT size to achieve the desired system performance. Also, the CD-NOMA in a multi-user scenario proved to be a key enabler in 5G to utilise the spectrum efficiently. This system can be further evaluated by increasing the number of users in a massive MIMO scenario.

REFERENCES

- [1] Technical Specification: Service Requirements for the 5G System. TS 22.261 V16.12.0. 2020.
- [2] P. Popovski, K. F. Trillingsgaard, O. Simeone, and G. Durisi, "5G wireless network slicing for eMBB, URLLC, and mMTC: A communication theoretic view," *IEEE Access*, vol. 6, pp. 55765–55779, Sep. 2018. <https://doi.org/10.1109/ACCESS.2018.2872781>
- [3] S. Gallenmuller, J. Naab, I. Adam, and G. Carle, "5G URLLC: A case study on low-latency intrusion prevention," *IEEE Commun. Mag.*, vol. 58, no. 10, pp. 35–41, Oct. 2020. <https://doi.org/10.1109/MCOM.001.2000467>
- [4] B. S. Khan, S. Jangsher, A. Ahmed, and A. Al-Dweik, "URLLC and eMBB in 5G industrial IoT: A survey," *IEEE Open Journal of the Communications Society*, vol. 3, pp. 1134–1163, Jul. 2022. <https://doi.org/10.1109/OJCOMS.2022.3189013>
- [5] C. Bockelmann, N. K. Pratas, G. Wunder, S. Saur, M. Navarro, D. Gregoratti, G. Vivier, E. De Carvalho, Y. Ji, C. Stefanovic, and P. Popovski, "Towards massive connectivity support for scalable mMTC communications in 5G networks," *IEEE Access*, vol. 6, pp. 28969–28992, May 2018. <https://doi.org/10.1109/ACCESS.2018.2837382>
- [6] A. Mughees, M. Tahir, M. A. Sheikh, and A. Ahad, "Energy-efficient ultra-dense 5G networks: Recent advances, taxonomy and future research directions," *IEEE Access*, vol. 9, pp. 147692–147716, Oct. 2021. <https://doi.org/10.1109/ACCESS.2021.3123577>
- [7] T. Kebede, Y. Wondie, J. Steinbrunn, H. B. Kassa, and K. T. Komegay, "Multi-carrier waveforms and multiple access strategies in wireless networks: Performance, applications, and challenges," *IEEE Access*, vol. 10, pp. 21120–21140, Feb. 2022. <https://doi.org/10.1109/ACCESS.2022.3151360>
- [8] L. Dai, B. Wang, Y. Yuan, S. Han, I. Chih-Lin, and Z. Wang, "Non-orthogonal multiple access for 5G: Solutions, challenges, opportunities, and future research trends," *IEEE Commun. Mag.*, vol. 53, no. 9, pp. 74–81, Sep. 2015. <https://doi.org/10.1109/MCOM.2015.7263349>
- [9] Z. Ding, P. Fan, and H. V. Poor, "Impact of user pairing on 5G nonorthogonal multiple-access downlink transmissions," *IEEE Trans. Veh. Technol.*, vol. 65, no. 8, pp. 6010–6023, Sep. 2016. <https://doi.org/10.1109/TVT.2015.2480766>
- [10] T. Cover, "Broadcast channels," *IEEE Trans. Inf. Theory*, vol. 18, no. 1, pp. 2–14, Jan. 1972.
- [11] S. Vanka, S. Srinivasa, Z. Gong, P. Vizi, K. Stamatiou, and M. Haenggi, "Superposition coding strategies: Design and experimental evaluation," *IEEE Trans. Wireless Commun.*, vol. 11, no. 7, pp. 2628–2639, May 2012. <https://doi.org/10.1109/TWC.2012.051512.111622>
- [12] N. I. Miridakis and D. D. Vergados, "A survey on the successive interference cancellation performance for single-antenna and multiple-antenna OFDM systems," *IEEE Commun. Surveys Tutorials*, vol. 15, no. 1, pp. 312–335, Feb. 2013. <https://doi.org/10.1109/SURV.2012.030512.00103>
- [13] V. Mojtaba *et al.*, "Interplay between NOMA and other emerging technologies: A survey," *IEEE Transactions on Cognitive Communications and Networking*, vol. 5, pp. 900–919, Aug. 2019. <https://doi.org/10.1109/TCCN.2019.2933835>
- [14] Z. Yang, Z. Ding, P. Fan, and N. Al-Dhahir, "A general power allocation scheme to guarantee quality of service in downlink and uplink NOMA systems," *IEEE Transactions on Wireless Communications*, vol. 15, no. 11, pp. 7244–7257, Nov. 2016. <https://doi.org/10.1109/TWC.2016.2599521>
- [15] M.-A. Seyed Hadi, V. Solouk, and H. Kalbkhani, "Energy-efficient user pairing and power allocation for granted uplink-NOMA in UAV communication systems," *Journal of Information Systems and Telecommunication*, vol. 10, no. 40, pp. 312–323, 2022. <https://doi.org/10.52547/jist.27369.10.40.312>
- [16] A. Kumar, K. Kumar, M. S. Gupta, and S. Kumar, "A survey on NOMA techniques for 5G scenario," in *Proceedings of the International Conference on Advances in Electronics, Electrical & Computational Intelligence (ICAEEC)*, Allahabad, India, May–June 2019, pp. 1–13. <https://doi.org/10.2139/ssrn.3573579>
- [17] Y. Tao, L. Liu, S. Liu, and Z. Zhang, "A survey: Several technologies of non-orthogonal transmission for 5G," *China Communications*, vol. 12, no. 10, pp. 1–15, Oct. 2015. <https://doi.org/10.1109/CC.2015.7315054>
- [18] T. Vakilian, F. Wild, F. Schaich, S. ten Brink, and J.-F. Frigon, "Universal-filtered multi-carrier technique for wireless systems beyond LTE," in *Proc. IEEE Globecom Workshops (Gc Wkshps)*, Atlanta, GA, USA, Dec. 2013, pp. 223–228. <https://doi.org/10.1109/GLOCOMW.2013.6824990>
- [19] S. Wei, H. Li, W. Zhang, and W. Cheng, "A comprehensive performance evaluation of universal filtered multi-carrier technique," *IEEE Access*, vol. 7, pp. 81429–81440, Jun. 2019. <https://doi.org/10.1109/ACCESS.2019.2923774>
- [20] L.E. Ghorab, E.F. Badran, A.I. Zaki, and W.K. Badawi, "Multicarrier technique for 5G massive MIMO system based on CDMA and CMFB," *Opt. Quant. Electron.*, vol. 55, 2023, Art. no. 25. <https://doi.org/10.1007/s11082-022-04272-9>
- [21] S. Adebisi and S. Oyetunji, "Data rate profiles of coded/uncoded power line channel with single-carrier/multicarrier modulation techniques," *Electrical, Control and Communication Engineering*, vol. 14, no. 1, pp. 23–29, Jul. 2018. <https://doi.org/10.2478/ecce-2018-0003>
- [22] A. Kumar and P. Vardhan, "Design, simulation & concept verification of 4 × 4, 8 × 8 MIMO with ZF, MMSE and BF detection schemes," *Electrical, Control and Communication Engineering*, vol. 13, no. 1, Dec. 2017. <https://doi.org/10.1515/ecce-2017-0010>
- [23] A. Bensky, "Introduction to information theory and coding," in *Short-range Wireless Communication* (3rd ed.), 2019, pp. 211–236. <https://doi.org/https://doi.org/10.1016/B978-0-12-815405-2.00009-9>

- [24] B. Das, M.P. Sarma, and K.K. Sarma, "Different aspects of interleaving techniques in wireless communication," in *Intelligent Applications for Heterogeneous System Modeling and Design*, IGI Global, 2015, pp. 335–374. <https://doi.org/10.4018/978-1-4666-8493-5.ch015>
- [25] M. Al-Imari and M. A. Imran, "Low density spreading multiple access," in *Multiple Access Techniques for 5G Wireless Networks and Beyond*, M. Vaezi, Z. Ding, and H. Poor, Eds. Springer, Cham, 2019, pp. 493–514. https://doi.org/10.1007/978-3-319-92090-0_15
- [26] N. H. Trung, "Multiplexing techniques for applications based-on 5G systems," in *Multiplexing – Recent Advances and Novel Applications*. London, United Kingdom: IntechOpen, 2022. <https://doi.org/10.5772/intechopen.101780>
- [27] M. Elkourdi, B. Peköz, E. Güvenkaya, and H. Arslan, "Waveform design principles for 5G and beyond," in *2016 IEEE 17th Annual Wireless and Microwave Technology Conference (WAMICON)*, Clearwater, FL, USA, Apr. 2016, pp. 1–6. <https://doi.org/10.1109/WAMICON.2016.7483859>
- [28] Y. Liu, X. Chen, Z. Zhong, B. Ai, D. Miao, Z. Zhao, J. Sun, Y. Teng, and H. Guan, "Waveform design for 5G networks: Analysis and comparison," *IEEE Access*, vol. 5, pp. 19282–19292, Feb. 2017. <https://doi.org/10.1109/ACCESS.2017.2664980>
- [29] S. Nagul, "A review on 5G modulation schemes and their comparisons for future wireless communications," in *Proc. Conf. Signal Process. Commun. Eng. Syst. (SPACES)*, Vijayawada, India, Jan. 2018, pp. 72–76. <https://doi.org/10.1109/SPACES.2018.8316319>
- [30] A. Qasim, M. A. Karabulut, H. Ilhan, and M. B. Islam, "Survey and performance evaluation of multiple access schemes for next-generation wireless communication systems," *IEEE Access*, vol. 9, pp. 113428–113442, Aug. 2021. <https://doi.org/10.1109/ACCESS.2021.3104509>
- [31] H. Zhang, H. Lv, and P. Li, "Spectral efficiency analysis of filter bank multi-carrier (FBMC)-based 5G networks with estimated channel state information (CSI)," *Towards 5G Wireless Netw. Phys. Layer*, vol. 26, pp. 49–82, Dec. 2016. <https://doi.org/10.5772/66057>
- [32] A. Farhang, N. Marchetti, F. Figueiredo, and J. P. Miranda, "Massive MIMO and waveform design for 5th generation wireless communication systems," in *1st International Conference on 5G for Ubiquitous Connectivity*, Dec. 2014, pp. 70–75. <https://doi.org/10.4108/icst.5gu.2014.258195>
- [33] F. Schaich, T. Wild, and Y. Chen, "Waveform contenders for 5G-suitability for short packet and low latency transmissions," in *Proceedings of the IEEE 79th Vehicular Technology Conference (VTC Spring)*, Seoul, Korea, May 2014, pp. 1–5. <https://doi.org/10.1109/VTCSpring.2014.7023145>
- [34] M.R. Abou Yassin, H. Abdallah, H. Issa, and S. Abou Chahine, "Universal filtered multi-carrier peak to average power ratio reduction," *Journal of Communications*, vol. 14, no. 3, pp. 243–248, Mar. 2019. <https://doi.org/10.12720/jcm.14.3.243-248>
- [35] C. Nassar, "Chapter 7 – Channel coding and decoding: Part 2 – Convolutional coding and decoding," *Telecommunications Demystified*, 2001, pp. 197–219. <https://doi.org/10.1016/B978-0-08-051867-1.50013-5>
- [36] A. Mojtaba and A. Akhavan, "A novel detector based on compressive sensing for uplink massive MIMO systems," *Journal of Information Systems and Telecommunication (JIST)*, vol. 10, no. 40, pp. 249–256, 2022. <https://doi.org/10.52547/jist.34192.10.40.249>



Smita Jolania holds a Bachelor of Engineering (Hons.) in Electronics and Communication, and a Master of Technology in Digital Communication. She is a Research Scholar at the Institute of Engineering and Technology, DAVV, in the domain of Wireless Communication Networks, 5G and beyond Networks and Signal Processing. She has published various research papers on the wireless cellular network in international journals and conference proceedings. Currently, she is

working as an Assistant Professor at Medicaps University, with an experience of 13 years in academics.

E-mail: sprajapati2911@gmail.com

ORCID iD: <https://orcid.org/0000-0001-5124-0248>



Ravi Sindal received the B.E. (Hons) degree from Rajasthan University, Jaipur in 1998. He received the M. Tech. degree in Instrumentation and PhD degree in Electronics and Telecommunication from Devi Ahilya University in 2000 and 2011, respectively. Since 2013, he has been a Professor of Electronics and Telecommunications at the Institute of Engineering and Technology, Devi Ahilya University, Indore. His research interests include radio resource management, modelling and simulation, digital design, and wireless networks. He has served on the program committee of various conferences. He has published many papers in various reputed international journals and conference proceedings.

E-mail: rsindal@ietdavv.edu.in



Ankit Saxena, (Senior Member, IEEE), holds an engineering diploma in Electronics Communication, a Bachelor of Engineering in Electronics and Instrumentation, a Master of Business Administration (System), and a Master of Electronics Engineering (Electronics and Telecommunication Engineering). Currently, he focuses on the Disruption of 5G/NB-IOT and RF in Telecom and Energy Utilities. He had a variety of positions at Ericsson, Alcatel-Lucent, Reliance Communications, and Tata Teleservices (TTSL),

where he contributed to the administration and enhancement of various communications networks. The Faculty of Engineering of DAVV University, Indore, has awarded him a PhD in Engineering (2018). He has published several research papers on wireless mobility in science citation index journals.

E-mail: ankitsaxena4u@gmail.com; dr.ankitsaxena@ieee.org